Induction of heme-oxygenase 1 requires the p38$^{\text{MAPK}}$ and PI3K pathways and suppresses apoptotic cell death following hypericin-mediated photodynamic therapy

**Silvia Kocanova · Esther Buytaert ·
Jean-Yves Matroule · Jacques Piette · Jakub Golab ·
Peter de Witte · Patrizia Agostinis**

Abstract Photodynamic therapy (PDT) is an established anticancer modality utilizing the photogeneration of reactive oxygen species (ROS) to kill the cancer cells and hypericin is a promising photosensitizer for the treatment of bladder tumors. In this paper we characterize the signaling pathways and the mechanisms leading to the up-regulation of the antioxidant enzyme heme oxygenase (HO-1) in PDT treated cancer cells. We show that PDT engages the p38$^{\text{MAPK}}$ and PI3K signaling cascades for HO-1 induction. p38$^{\text{MAPK}}$ inhibitors or small interfering RNA (siRNA) for p38$^{\text{MAPK}}$ suppress HO-1 induction after PDT and complete repression is attained when p38 and PI3K antagonists are combined. Blocking these signaling pathways increases additively the propensity of the cells to undergo PDT-induced apoptosis, mirroring the effect of HO-1 silencing. Conversely, increasing HO-1 protein level by hemin prior to irradiation is cyto-protective. HO-1 stimulation by PDT is dependent on transcription and *de novo* protein synthesis and it is preceded by the nuclear accumulation of the Nrf2 transcription factor, which is reduced by inhibitors of p38$^{\text{MAPK}}$ and PI3K. Altogether these results indicate that stimulation of HO-1 expression by hypericin-PDT is a cytoprotective mechanism governed by the p38$^{\text{MAPK}}$ and PI3K pathways, likely through the control of the nuclear availability of the Nrf2 pool.

Keywords HO-1 · Apoptosis · PDT · Hypericin · Reactive oxygen species · Cancer therapy · PI3K · p38MAPK · Nrf2

Abbreviations

ActD	actinomycin D
AREs	antioxidant response elements
B2M	β2-microglobulin
COX-2	cyclooxygenase-2
ER	endoplasmic reticulum
HO-1	heme oxygenase 1
Hyp	Hypericin
Nrf2	NF-E2-related factor-2
p38$^{\text{MAPK}}$	p38 mitogen-activated protein kinase
PDT	photodynamic therapy
PGE$_2$	prostaglandin E$_2$
PI3K	phosphatidylinositol 3-kinase
ROS	reactive oxygen species
ZnPPIX	zinc protoporphyrin IX

S. Kocanova · E. Buytaert · P. Agostinis (✉)
Department Molecular and Cell Biology, Division of
Biochemistry, Catholic University of Leuven,
Campus Gasthuisberg, Herestraat 49,
B-3000 Leuven, Belgium
e-mail: Patricia.Agostinis@med.kuleuven.ac.be

P. de Witte
Laboratory for Pharmaceutical Biology and Phytopharmacology,
Catholic University of Leuven,
B-3000 Leuven, Belgium

J.-Y. Matroule · J. Piette
Laboratory of Virology and Immunology, Institute of Pathology
B23 University of Liège,
B-4000 Liège, Belgium

J. Golab
Department of Immunology, Center of Biostructure Research,
The Medical University of Warsaw,
Warsaw, Poland

1 Introduction

Photodynamic therapy (PDT) is an attractive therapeutic procedure suitable for the management of a variety of tumors and non-malignant disorders. PDT involves the administration of a photosensitizing compound (photosensitizer) which

preferentially accumulates in the tumor or in hyperproliferating tissue, followed by irradiation with visible light [1]. Light irradiation of the photosensitizing drug leads, in the presence of molecular oxygen, to the photogeneration of reactive oxygen species (ROS), which ultimately kill the target cells. PDT with the ER-localizing hypericin, a naturally occurring photosensitizer, causes rapid emptying of the ER-Ca^{2+} stores and cell death, which can be executed either in a caspase-dependent or in autophagy-dependent fashion [2]. The interesting photosensitizing properties of hypericin together with its selective uptake in tumor tissues, especially in bladder cancers, and its minimal dark cytotoxicity, hold promise for the clinical use of this sensitizer in the photodynamic treatment of cancers [3].

Although in general PDT has been found to be an efficient inducer of cell death, some *in vivo* studies indicate that PDT also activates rescuing pathways, which ultimately can lead to tumor survival and recurrence [4]. We have recently reported that following exposure of tumor cells to PDT different signal transduction pathways are engaged leading to the expression of the inducible cyclooxygenase-2 (COX-2) [5, 6], a master enzyme involved in the conversion of arachidonic acid to PGE_2, with a documented tumor promoting role [7]. In particular, up-regulation of the COX-2 protein levels by hypericin-PDT is mediated by the stabilization of the COX-2 transcript through the specific activation of the $p38^{MAPK}$ signaling pathway [5]. However, blocking COX-2 activity does not fully recapitulate the anti-apoptotic effects of the inhibition of $p38^{MAPK}$ after hypericin-PDT [5, 8], thus arguing that $p38^{MAPK}$ affects other targets which confer increased protection against the photo-oxidative injury. The identification of the molecular elements of the cellular rescue responses activated by hypericin-mediated PDT is of therapeutic importance as their inhibition is expected to enhance the tumoricidal efficacy of this anticancer strategy.

Heme oxygenase isozymes (HO-1 and HO-2) catalyze in mammalian cells the rate-limiting step in the catabolic degradation of heme yielding equimolar amounts of carbon monoxide (CO), iron and biliverdin. Biliverdin is further converted to bilirubin by the ubiquitous enzyme biliverdin reductase [9]. Several reports indicate that moderate levels of the heme-derived metabolites bilirubin and CO generated by HO-1 catalysis have potent antioxidant and cytoprotective actions, while free iron is rendered redox-inactive by effective ferritin sequestration [9]. Contrary to HO-2 which is expressed constitutively, the inducible HO-1 isozyme is a phase II enzyme that is commonly transcriptionally regulated in response to various cellular signals, although stabilization of HO-1 mRNA has been reported in some paradigms [10, 11]. The *ho-1* gene is induced by a variety of stimuli including pro-inflammatory cytokines, tumor promoters and certain growth factors, heavy metal salts, heat shock, hypoxia, and by agents and chemicals that produce oxidative

stress, including its substrate heme, sodium arsenite, hydrogen peroxide, glutathione depletion, nitric oxide, ultraviolet A (UVA; 320–380 nm) radiation [9]. Furthermore, studies using gene-knockout and transgenic mice have validated the biological role of HO-1 in anti-oxidant and adaptive inflammatory responses [12]. Relevant in this context, a recent report shows that HO-1 induction by photofrin-mediated PDT [13] significantly decreases the susceptibility of tumor cells to photokilling [14]. However, while it is widely accepted that induction of HO-1 expression represents an adaptive response that increases cell resistance to a variety of oxidative injuries, the molecular steps and the signal transduction pathways underlying HO-1 up-regulation in general, and by the photochemically generated ROS, in particular, remain largely undefined.

This study was undertaken to characterize at the molecular level the signaling pathway(s) promoting HO-1 upregulation by hypericin-mediated PDT, with particular emphasis on the participation of the $p38^{MAPK}$ as a possible positive regulator of HO-1 in our system. We show that in two different human cancer cell lines, e.g. HeLa and T24 cells, hypericin photosensitization results in a time- and dose-dependent up-regulation of HO-1 at both the RNA and protein levels. Induction of HO-1 by hypericin-PDT is reduced by the inhibition of $p38^{MAPK}$ and PI3K, and results in the increased resistance of the cells to the PDT stress. Our results also show that these signaling pathways contribute to the nuclear accumulation of the transcription factor Nrf2, which precedes up-regulation of HO-1 expression in our paradigm.

2 Materials and methods

2.1 Materials

Hypericin was prepared, purified, and dissolved in DMSO as described in [15]. All cell culture products were obtained from Cambrex (Verviers, Belgium), except fetal calf serum, which was from Perbio Hyclone (Erembodegem, Belgium). Anti-caspase-3, anti-HO-1, anti-phospho-Akt (Ser^{473}), anti-Akt and anti-Nrf2 antibodies were purchased from Santa Cruz Biotechnology (Santa Cruz, CA, USA). Anti-phospho-$p38^{MAPK}$ (Thr^{180}/Tyr^{182}) monoclonal antibody, which specifically recognizes the phosphorylated form of the kinase and anti-$p38^{MAPK}$ antibody were purchased from New England Biolabs, Inc. (Beverly, MA, USA). Monoclonal anti-α-tubulin antibody was from Sigma (Bornem, Belgium). The anti-CDC5L antibody which specifically recognizes the human homolog CDC5L of *Schizosaccharomyces pombe* cdc5, a regulator of pre-mRNA splicing, was a gift from Dr. Monique Beullens (KUL Biochemistry, Belgium).

Horseradish peroxidase-conjugated secondary antibodies were from DAKO (Denmark), whereas the Alexa Fluor® 488

goat anti-rabbit antibody was from Molecular Probes, Inc. (Eugene, OR). Hoechst 33342, actinomycin D, cycloheximide and hemin were from Sigma. The p38^{MAPK} inhibitor PD169316, the ERK inhibitor PD98059, the JNK inhibitor SP600125, the PKC inhibitors Gö6976 (PKC-α and -β) and Gö6983 (PKC-α, -β, -γ, -δ and -ζ) were purchased from Calbiochem (San Diego, CA, USA), whereas the specific inhibitor of PI3-kinase LY294002 was from Cell Signaling Technology (Danvers, MA) and the specific peptide inhibitor (PKI) towards PKA was a gift from Dr. Monique Beullens (KUL Biochemistry, Belgium).

Small interfering RNA (siRNA), *ho-1* siRNA, p38 siRNA and nontargeting negative control siRNA, as well as all reagents for the siRNA transfection were purchased from Dharmacon (Lafayette, USA).

2.2 Cell culture and photosensitization

HeLa cells (human cervix carcinoma cells) and T24 (human transitional cell carcinoma of the urinary bladder) were cultured as described in [16]. T24 or HeLa cells were pre-incubated with hypericin for 16 h, in subdued light conditions (< 1 μW/cm^2) and subsequently irradiated in Dulbecco's modified Eagle's medium by placing the samples on a plastic diffuser sheet 5 cm above a set of seven L18W30 fluorescent lamps (Osram; maximal emission between 530 and 620 nm, coinciding with the absorption peak of hypericin at 595 nm). At the surface of the diffuser, the uniform fluence rate was 4.5 mW/cm^2, as measured with an IL 1400 radiometer (International Light, Newburyport, MA). The fluence or light dose (J/cm^2) was calculated by multiplying the fluence rate with the time of irradiation. Actinomycin D, cycloheximide and all inhibitors used were added to the cell culture medium 1 h prior to photosensitization at concentrations indicated in the figure legends. After 1 h of incubation the medium was changed with complete Dulbecco's modified Eagle's medium and cells were irradiated as described above. After irradiation the medium with desired components was readded for next hours till the end of experiment.

For the experiment with hemin, T24 and HeLa cells were co-incubated with or without 150 nM and 125 nM hypericin, respectively, and 5 μM hemin for 16 h. After indicated time incubation the medium was changed with complete Dulbecco's modified Eagle's medium, cells were irradiated and 7 h after irradiation prepared for Western blot or cell death analysis.

2.3 Preparation of cell extracts and Western Blotting

Preparation of cell extracts at the indicated time points following photosensitization and Western blotting were performed as described previously [16].

2.4 Preparation of nuclear fractions

T24 cells (1×10^6) were washed with ice-cold PBS, scraped and centrifuged at 1,500 $\times$ g for 5 min at 4°C. The pellets were resuspended in 100 μl digitonin lysis buffer containing 1% digitonin and 1 mM EDTA in PBS, immediately centrifuged at 13,000 $\times$ g for 20 min at 4°C. The pellets were resuspended in 100 μl HEPES lysis buffer containing 1% Triton X-100, 10% glycerol, 10 μg/ml leupeptin, 5 μg/ml aprotinin, 1 mM PMSF, 1 mM Na$_3$VO$_4$ and 50 mM NaF in HEPES buffer (20 mM HEPES, 0.3 M NaCl, 1.5 mM MgCl$_2$, 20 mM β-glycerol-phosphate, 2 mM EDTA, 2 mM EGTA and 1 mM DTT), kept 15 min on ice and centrifuged at 13,000 $\times$ g for 15 min at 4°C. Supernatants of these nuclear lysates were saved as nuclear fractions and stored at -70°C until use. Protein concentrations were determined using the Bio-Rad Protein Assay (Bio-Rad).

2.5 Cell death assay

T24 and HeLa cells were treated as described before. At the indicated time points, the cells were washed with ice-cold PBS, fixed in 10% paraformaldehyde in PBS for 30 min at room temperature. After washing with PBS, the cells were permeabilized with cold methanol for 10 min at room temperature, washed three times with PBS and stained with Hoechst 33342 (1:1000 in PBS) for 15 min at room temperature. The sample was then examined using fluorescence microscopy Diaplan, Leitz, Germany. Apoptotic nuclei were counted and expressed as percentage of apoptotic nuclei over the total number of nuclei. At least 10 fields with a minimum of 50 cells were counted.

2.6 Immunofluorescence microscopy

T24 cells, plated on six-well plates, were washed with ice-cold PBS and fixed in 10% paraformaldehyde in PBS for 30 min at room temperature, at indicated time points after the treatment. Cells were then washed with PBS, permeabilized with cold methanol for 10 min at room temperature and washed three times with PBS. After blocking for 3 h in PBS containing 1% bovine serum albumin, the cells were washed once with PBS for 5 min and incubated overnight at 4°C with anti-Nrf2 antibody (1:500 in 1% bovine serum albumin in PBS) followed, after washing, by incubation with the Alexa Fluor® 488 goat anti-rabbit antibody for 90 min in the dark at room temperature. Preparations were then counterstained for 15 min with Hoechst 33342 (1:1000 in PBS) in the dark at room temperature, to stain the nuclei. After washing with PBS, the samples were examined by fluorescence microscopy (Diaplan, Leitz, Germany) equipped with a Zeiss oil-immersion objective (100 $\times$) and a digital camera (DC 200, Leica Microsystems, Wetzlar, Germany). Nrf2 was

visualized using the filter set containing BP 450–490 and LP 515 for excitation and emission, respectively. Hoechst 33342 was visualized using the filter set containing BP 340–380 and LP 425. All filters were from Leica Microsystems.

2.7 Cell transfection with siRNA

T24 cells were transfected either with 200 nM siRNA SMARTpool® p38^MAPK or 100 nM siRNA SMARTpool® *ho-1* (Upstate/Dharmacon, Waltham, MA) or Negative Control siRNA Alexa Fluor 488 (Qiagen, Venlo, Netherlands) using Oligofectamine™ Reagent (Invitrogen, Carlsbad, CA) according to manufacturer's instructions. Briefly, the cells were plated one day before transfection in complete Dulbecco's modified Eagle's medium without antibiotics. Next day, the cells were washed with serum free Dulbecco's modified Eagle's medium, and complex containing oligonucleotide and oligofectamine in serum free Dulbecco's modified Eagle's medium was added. The cells were incubated for 4 h with complex in serum free medium and next, complete Dulbecco's modified Eagle's medium was supplemented to obtain final 10% FCS. Preliminary studies showed that maximal p38^MAPK and HO-1 protein knockdown occurred 3 days after transfection using 200 nM p38 siRNA or 100 nM HO-1 siRNA.

2.8 Quantitative RT-PCR

cDNA were prepared in a 20 μl final volume with 1 μg RNA as described in [6]. 2 μl cDNA were mixed with 10 μl SYBR Green Mix (Applied Biosystems, Warrington, UK) and with 270 nM forward (5′ CTGAGTTCATGAGGAACTTTCA-GAAG 3′) and 270 nM reverse (5′ TGGTACAGGGAGGC-CATCAC 3′) HO-1 primers or with 300 nM forward (5′ GAGTATGCCTGCCGTGTG 3′) and 300 nM reverse (5′ AATCCAAATGCGGCATCT 3′) β2-microglobulin (B2M) primers in a 20 μl final volume. Real-time PCR was performed with the ABI-PRISM 7000 Sequence Detection System (Applied Biosystems, Warrington, UK). Data were subjected to relative quantification using the comparative C_T ($\Delta\Delta C_T$) method where B2M was used as an endogenous reference for normalization. The following arithmetic formula was applied to each sample and the results plotted in fold induction: $2^{-(CT_{treated}-CT_{untreated})HO-1 \, - \, (CT_{treated}-CT_{untreated})B2M}$.

3 Results

### 3.1 Hypericin-PDT induces HO-1 at the mRNA and protein levels in human cancer cells

We first evaluated whether PDT with hypericin results in the up-regulation of HO-1 at the protein and mRNA levels using
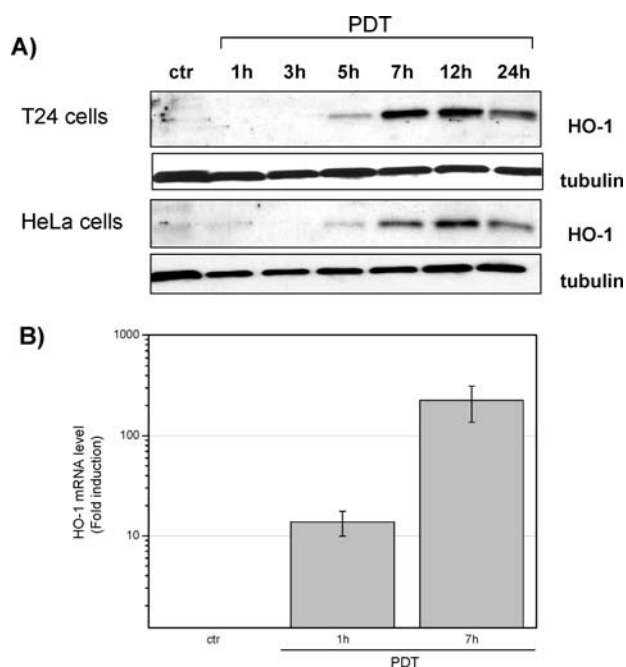
Fig. 1 Induction of HO-1 at the protein and RNA levels in hypericin-PDT treated cells. T24 and HeLa cells were incubated with 150 nM or 125 nM hypericin, respectively, for 16 h and then irradiated (4 J/cm²). (A) Untreated (ctr; hypericin without irradiation) and PDT-treated cells were harvested at the indicated time points after irradiation and subjected to Western blot analysis using anti-HO-1 or anti-α-tubulin antibodies, respectively. (B) Total RNA was extracted from untreated and PDT-treated T24 cells 1 h and 7 h post-irradiation. HO-1 mRNA level was analyzed by RT-PCR. *Error bars* represent S.D. of two independent experiments

the human cancer cell lines T24 (TCC of the bladder) and HeLa (cervix carcinoma) as preferential model systems. Incubation of T24 or HeLa cells with hypericin (125 or 150 nM) followed by irradiation (4 J/cm²) induced HO-1 protein expression in time-dependent manner as detected by Western blot analysis (Fig. 1(A)). Kinetic experiments showed that induction of HO-1 protein expression in response to hypericin-PDT was readily detectable 5 h after irradiation and persisted over 24 h, reaching an apparent maximal induction 7 h in T24 and 12 h in HeLa cells after PDT exposure (Fig. 1(A)). Induction of HO-1 was specifically dependent on the concomitant presence of hypericin and light, as either hypericin (Fig. 1(A)) or light alone (not shown) did not induce any response. Consistent with the corresponding increase in the HO-1 protein expression quantitative RT-PCR in T24 cells revealed an induction of HO-1 mRNA as early as 1 h post-irradiation, which increased dramatically 7 h after PDT (Fig. 1(B)).

Stimulation of HO-1 protein expression was induced by light activation of hypericin in a concentration range resulting in approximately 70% (e.g. mildly lethal PDT conditions with 75 nM hypericin) or 20% (e.g. lethal PDT condition with 150 nM hypericin leading to apoptotic cell death) survival (data not shown).
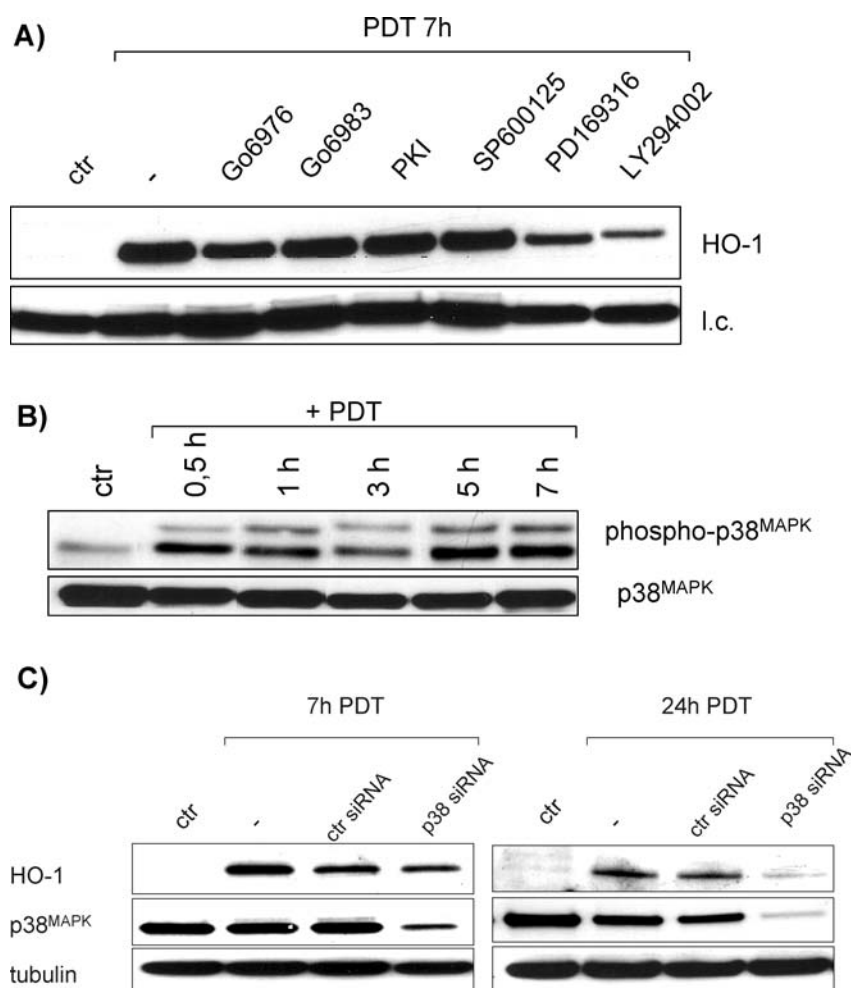
Fig. 2 Blocking p38 $^{\text{MAPK}}$ and PI3K prevents HO-1 up-regulation after hypericin-PDT. (A) T24 were preincubated for 1 h with either 200 nM Gö6976, 200 nM Gö6983, 0.6 μM PKI, 1 μM SP600125, 1 μM PD169316, or 10 μM LY294002, as indicated. Cells were left untreated (ctr) or treated by PDT (150 nM Hyp and 4 J/cm^2 irradiation). Protein extracts were prepared 7 h after irradiation and analyzed by Western blotting with specific antibodies for HO-1. (B) T24 cells were incubated for 16 h with 150 nM hypericin and then irradiated (4 J/cm^2). At the indicated time points after irradiation, the activity and protein level of p38$^{\text{MAPK}}$ were analyzed by Western blot with specific anti-phospho- or anti-p38$^{\text{MAPK}}$ antibodies. A representative picture is shown. (C) T24 cells were transfected with p38 siRNA 72 h before treatment (as described under "Materials and Methods") and incubated for 16 h with 150 nM Hyp. Untreated and PDT-treated cells were harvested 7 h and 24 h following irradiation and subjected to Western blot analysis using anti-HO-1, anti-p38$^{\text{MAPK}}$ and anti-α-tubulin antibodies, respectively. Results shown are representative of at least 3 independent experiments

3.2 Induction of HO-1 by PDT requires the p38$^{\text{MAPK}}$ and PI3K pathways

Accumulating evidence indicates that many inducers of HO-1 activate protein phosphorylation-dependent signaling cascades that ultimately converge to the transcription factors regulating the *ho-1* gene [9]. The three major members of the MAPK cascades, ERK, JNK and p38$^{\text{MAPK}}$, have been, either alone or in combination, principally implicated in *ho-1* activation, though pathways mediated by the phosphatidylinositol 3-kinase (PI3K), PKA and PKCs, have also been documented [9]. In order to evaluate the participation of these signaling cascades in our paradigm we initially employed pharmacological or peptide inhibitors (i.e., p38$^{\text{MAPK}}$:

PD169316; MEK1: PD98059, JNK: SP600125: PKC-α, -β: Gö6976 and PKC-α,-β, -γ, -δ,-ζ; Gö6983, PKA: PKI, PI3K: LY294002/wortmannin) of these protein kinases and assessed their effects on HO-1 induction by hypericin-PDT. Stimulation of HO-1 expression by PDT was unaffected by antagonists of the ERK- (data not shown), PKC (α, -β,-γ, -δ,-ζ isoforms)-, PKA- and JNK-pathways, thus ruling out the contribution of these kinase signaling cascades in our conditions (Fig. 2(A)). Conversely, pretreatment of T24 cells with inhibitors of the p38$^{\text{MAPK}}$ α and β isoforms (1 μM PD169316) and of the phospholipid kinase PI3K (10 μM LY294002), resulted in a significant reduction of the stimulation of HO-1 expression by PDT (Fig. 2(A)). Similar results were observed in HeLa cells (data not shown), thus

suggesting a general requirement of these signal transduction pathways for HO-1 protein up-regulation in our PDT paradigm.

The kinetics of activation of p38[MAPK] and Akt, as a downstream effector of PI3K were monitored by the use of activation-specific antibodies that selectively recognize the active and phosphorylated forms of p38[MAPK] and Akt (Ser[473]). Although, as reported in previous studies [5, 29], p38[MAPK] activation in photosensitized cells clearly preceded the stimulation of HO-1 protein expression (Fig. 2(B)), we failed to observe a significant and persistent activation of Akt in both T24 and HeLa cells (data not shown). Moreover, overexpression of a constitutively active Akt mutants in HeLa cells did not influence HO-1 expression after PDT (data not shown), thus suggesting that PI3K regulates HO-1 by a mechanism independent on Akt.

Given the important role of the p38[MAPK] pathway in hypericin-PDT in T24 cells [5, 6] we found it imperative to add evidence confirming HO-1 as a potential p38[MAPK] downstream target in our paradigm. To this end we silenced the expression of p38[MAPK] in T24 cells, subjected them to the photodynamic treatment and monitored the expression of HO-1 as a function of time. As shown in Fig. 2(C), when p38[MAPK] expression was knocked down with a p38-specific small interfering RNA (siRNA) we observed a direct relationship between the decreased level of p38[MAPK] expression and abolition of HO-1 stimulation by PDT. These data thus demonstrate that HO-1 is a genuine target of the p38[MAPK] pathway.

3.3 Inhibition of the p38[MAPK] and PI3K cascades following PDT counteracts the cytoprotective effect of HO-1 up-regulation

Next, we evaluated the effect of blocking the PI3K or the p38[MAPK] -pathways either alone or in combination, on the extent of apoptosis in T24 exposed to PDT. Inhibition of either p38[MAPK] or PI3K by PD169316 or LY294002, respectively, resulted in an increased amount of cells containing Hoechst 33342-detectable chromatin condensation as compared to PDT treated cells in the absence of the pharmacological inhibitors (Fig. 3(A)). Notably, the simultaneous addition of both antagonists prior to PDT increased the susceptibility to apoptotic cell death in an additive fashion, thus supporting a cytoprotective role for both pathways in our paradigm (Fig. 3(A)). It should be noted that the control cells (e.g. not irradiated, Fig. 3(A)) incubated with PD169316 or LY294002, either alone or in combination, did not manifest any sign of cytotoxicity, thus arguing that these inhibitors block PDT-induced survival pathways. Furthermore, their additive effect on apoptotic cell death correlated well with the ablation of HO-1 expression following PDT when both pharmacological inhibitors were used together, suggesting a correlation between reduced HO-1 expression and increased
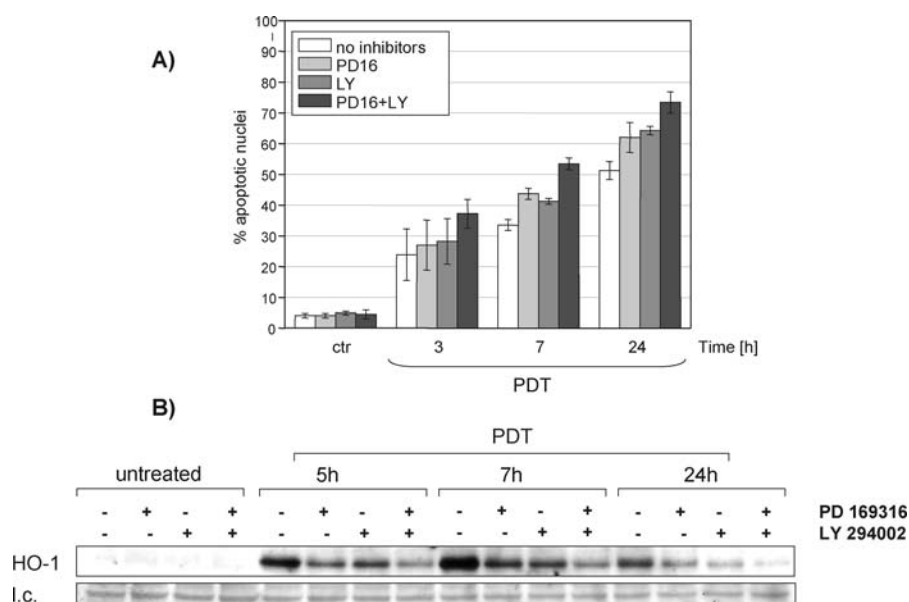
Fig. 3 HO-1 is modulated by the anti-apoptotic p38 [MAPK] and PI3K pathways. T24 cells were incubated with 150 nM hypericin for 16 h and pretreated for 1 h with 1 μM PD169316 and/or 10 μM LY294002 before being exposed to irradiation (4 J/cm^2; PDT) or not (ctr). (A) At the indicated time points following irradiation, cells were stained with Hoechst 33342 and the percentage of apoptotic cells was determined by counting the number of cells showing apoptotic morphology over the total cell number, as calculated in at least 10 independent fields. Control cells did not show measurable differences during the entire time course. *Error bars* represent S.D. of two independent experiments. (B) In parallel experiments, cell lysates were prepared at the indicated time points and subjected to immunoblot analysis using anti-HO-1 antibodies

Fig. 4 Induction of HO-1 protects cells from photokilling. (A) T24 and ▶ HeLa cells were pretreated with 150 nM or 125 nM hypericin respectively and 5 μM hemin as indicated, for 16 h. The cells were then either irradiated (4 J/cm^2) or left untreated (ctr) and harvested 7 h afterwards. Cell lysates were analysed for HO-1 protein level by Western blotting with specific anti-HO-1 antibodies. (B) In a parallel experiment cells were fixed with 10% paraformaldehyde, stained with Hoechst 33342 (1:1000 in PBS) and visualized by fluorescent microscopy. The percentage of apoptotic cells was determined as described under "Materials and Methods". Representative pictures are shown *(inset)*: untreated (a, b) and PDT-treated (c, d) cells without (a, c) or with (b, d) 5 μM hemin. (C) T24 cells were pretreated with HO-1 siRNA for 72 h, 16 h with 150 nM hypericin and 1 h before irradiation with 1 μM PD169316, as described under "Materials and Methods". At the indicated time point after irradiation, cells were harvested and analyzed for the presence of HO-1 protein level, as well as caspase-3 cleavage by Western blot using specific anti-HO-1 and anti-caspase-3 antibodies. (D) In a parallel experiment cells were fixed with 10% paraformaldehyde, stained with Hoechst 33342, nuclear condensation was visualized by fluorescent microscopy and the percentage of apoptotic nuclei was determined as described under "Materials and Methods". Results shown are representative of at least 3 independent experiments


cellular propensity to undergo photokilling (Fig. 3(B)). Indeed, while inhibition of either the p38^{MAPK} or PI3K pathway in cell exposed to PDT blunted HO-1 protein expression by approximately 50–60% after 7 h, when PD169316 and LY294002 were used together the HO-1 expression by PDT was completely prevented (Fig. 3(B))

Up-regulation of HO-1 expression by its substrate hemin has been reported to protect cells from oxidative injury [14, 17]. Thus, to establish further a causative link between HO-1 expression and resistance to hypericin-PDT induced apoptosis, we interfered with the expression of HO-1 in T24 cells through a pharmacological and RNAi approach.

First we addressed the question as to whether cell pretreatment with hemin, as an endogenous inducer of HO-1 expression, prior to PDT would result in an increased cytoprotection from the subsequently photogenerated ROS. Consistent with previous reports, pretreatment of the cells with hemin for 16 h stimulated HO-1 expression and further exposure of the cells to PDT resulted in an additional increase in HO-1 protein levels (Fig. 4(A)), which persisted up to 24 h after PDT (data not shown). Cells pretreated with hemin were less prone to undergo subsequent PDT- induced apoptosis as compared to untreated cells containing undetectable HO-1 protein expression level (Fig. 4(B)). It should be noted that hemin did not induce p38^{MAPK} activation nor did it affect the PDT-mediated p38^{MAPK} activation (data not shown), thus indicating that HO-1 induction by hemin or by PDT involves different mechanisms.

Secondly, we assessed the effect of HO-1 suppression on photokilling. Since under our conditions the HO-1 inhibitor ZnPPIX exhibited cytotoxic effects (data not shown) when used in the concentrations range described in several studies to inhibit HO-1 activity [14, 18], we evaluated the
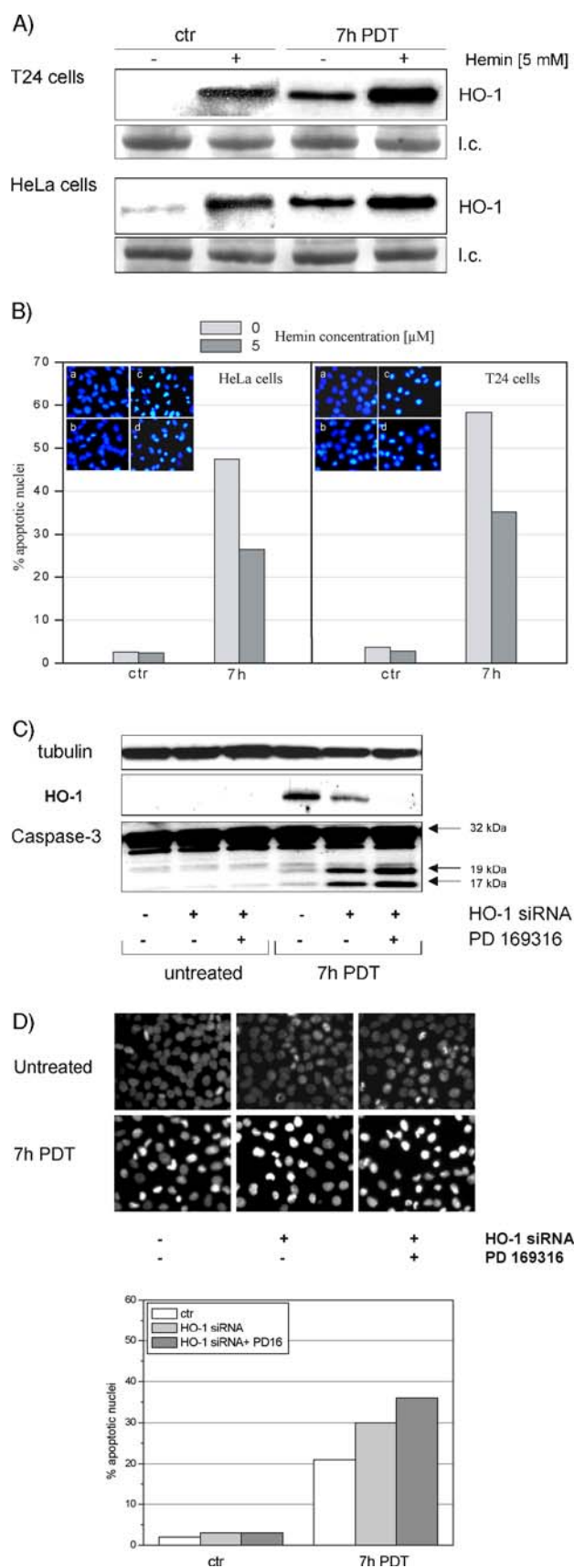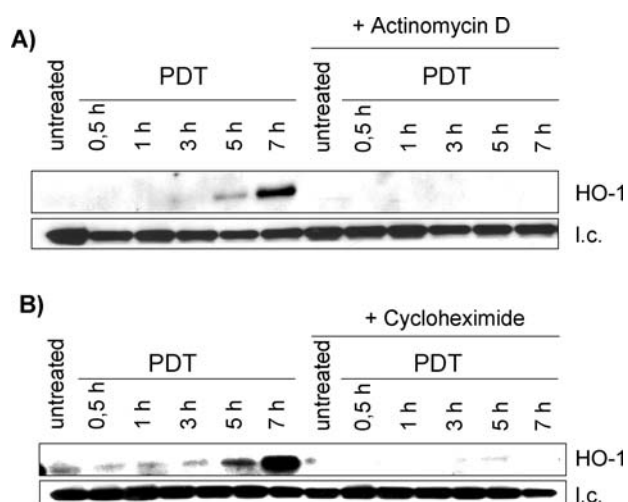
Fig. 5 HO-1 induction by PDT requires transcription and *de novo* protein synthesis. T24 cell were incubated with or without 150 nM hypericin for 16 h. (A) Actimomycin D (3 μg/ml) or (B) cycloheximide (10 μg/ml) was added to cells for 1 h before irradiation (as described under "Materials and Methods"). The cells were harvested and lysed 7 h after irradiation. HO-1 protein levels were determined by Western blot analysis

effect of HO-1 silencing in the T24 cells. Figure 4 shows that knocking down HO-1 protein levels after transfection of the T24 cells with an HO-1 siRNA resulted in an enhancement of caspase-3 cleavage (Fig. 4(C)) and nuclear condensation (Fig. 4(D)), two key apoptotic parameters, after PDT. Moreover, co-treatment of HO-1 silenced cells with PD169316 resulted in a complete shutdown of the HO-1 signal after PDT and in a further increase in the level of caspase-3 processing and chromatin condensation. Altogether these data indicate that an important mechanism by which the p38^{MAPK} and probably also the PI3K, pathway exert a cytoprotective effect after PDT is by stimulating the induction of HO-1.

3.4 HO-1 expression by PDT is preceded by the nuclear accumulation of Nrf2

In several systems the induction of HO-1 has been demonstrated to be a consequence of *de novo* transcription [9]. Thus, to explore the contribution of a transcriptional mechanism of HO-1 induction by PDT, we investigated the effect of the transcription inhibitor actinomycin D (ActD). As shown in Fig. 5(A), addition of ActD in T24 cells 1 h prior to irradiation completely blunted the induction of HO-1 expression in response to hypericin-PDT, thus indicating that active transcription is required for HO-1 expression in our paradigm. We were unable to determine the effect of ActD in HeLa cells, since in these cells the addition of this inhibitor was toxic after few hours of incubation (data not shown).

Furthermore, to determine the relevance of *de novo* protein synthesis in HO-1 induction by PDT, the cells were treated with the translation elongation inhibitor cycloheximide before irradiation. Pre-treatment of the cells with cycloheximide blocked the induction of HO-1 by PDT (Fig. 5(B)), thus indicating that HO-1 up-regulation is mediated by a mechanism requiring *de novo* protein synthesis as well.

Nrf2 (NF-E2-related factor-2), a member of the Cap'n'Collar family of transcription factors, has been implicated in the expression of phase II genes, including HO-1, through the regulation of antioxidant response elements (AREs) in response to a variety of stimuli [19]. Under non-stressed conditions, Nrf2 transactivation activity is repressed by binding to Keap1, an actin-binding protein which targets Nrf2 to degradation by the ubiquitin-proteasome pathway, thus maintaining low cellular Nrf2 levels [19, 20]. Following oxidative stress the Keap1-Nrf2 association is disrupted and Nrf2 is free to stabilize and to accumulate in the nucleus, where it can induce the expression of a set of cytoprotective genes. As PDT is a strong inducer of ROS, especially in the form of the non-radical but highly reactive $^1O_2$, we sought to determine whether hypericin-mediated photosensitization induced a time-dependent nuclear accumulation of Nrf2 in T24 cells. To this end, the cells were treated with PDT and at various time points after irradiation they were fixed, permeabilized and subjected to immunocytochemistry. In untreated cells detection of Nrf2 was found weak (Fig. 6(A)), suggesting that the pool of Nrf2 in non-stressed cells is small. Conversely, soon after irradiation Nrf2 became largely nuclear (Fig. 6(A)). The kinetics of Nrf2 nuclear accumulation clearly preceded HO-1 expression by PDT (see Fig. 1(A)), suggesting that *ho-1* could be regulated by Nrf2 in our paradigm.

We then addressed the kinetics of Nrf2 nuclear accumulation by mean of Western blot analysis after isolation of the nuclear fraction from untreated or PDT treated cells. The pattern of nuclear accumulation as detected by immunoblot mirrored kinetically the results of the immuncytochemistry in as much as we observed that Nrf2 accumulated in a time-dependent fashion in the nucleus while in non-stressed cells Nrf2 levels were very low. Importantly, inhibition of p38^{MAPK} or PI3K hampered Nrf2 nuclear accumulation induced by hypericin-PDT, as at all time points after PDT the detectable amount of nuclear Nrf2 was reduced in the presence of the pharmacological antagonists of these pathways (Fig. 6(B)).

Altogether these observations suggest that the p38^{MAPK} and PI3K pathways mediate the induction of HO-1 following PDT by modulating the nuclear accumulation of the redox-sensitive Nrf2 transcription factor, which is in turn required for the transcriptional activation of the cytoprotective *ho-1* gene.
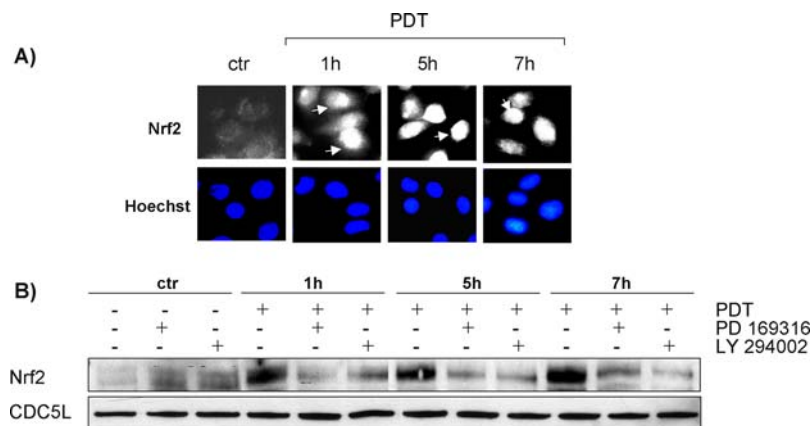
Fig. 6 PDT induced Nrf2 nuclear accumulation is reduced by p38^{MAPK} and PI3K inhibition. (A) T24 cells were incubated for 16 h with 75 nM hypericin and then irradiated (4 J/cm^2). At the indicated time points the cells were fixed, incubated with anti-Nrf2 antibodies overnight and then stained with Alexa Fluor$^®$ 488 goat anti-rabbit antibodies. Additionally, the cells were counterstained with second dye - Hoechst 33342 to stain the nuclei, as described under "Materials and Methods". The images were collected using flurescence microscopy Diaplan, Leitz, Germany. Pictures are representative of at least three independent ex-

periments. (B) T24 cells were incubated with 150 nM hypericin for 16 h and pretreated 1 h before irradiation (4 J/cm^2) with 1 μM PD169316 or 10 μM LY294002. Nuclear fractions of untreated (ctr) and PDT-treated cells for the indicated times were isolated as described under "Materials and Methods". Nuclear content of Nrf2 was analyzed by Western blot by anti-Nrf2 antibodies (Santa Cruz). The specific nuclear protein CDC5L [28] indicates equal loading. Results shown are representative of at least 3 independent experiments

4 Discussion

It has been recently established that cell responds to electrophiles and reactive oxygen species by activating a set of stress-responsive genes involved in cellular protection through the transcriptional activation of the antioxidant response element (ARE). ARE is a *cis*-acting regulatory element in promoter regions of several genes encoding antioxidant and Phase II drug-metabolizing enzymes [21]. The inducible antioxidant enzyme HO-1 is among genes that contain a functional ARE, and which also include NAD(P)H:quinone reductases (NQO1), γ-glutamyl cysteine ligase (γ-GCL) and ferritin among others [22]. Intriguingly, global gene expression analysis of the bladder cancer cell line T24 treated with hypericin-PDT has revealed that this battery of ARE-regulated genes, and most dramatically of all the HO-1, is induced in a coordinated manner (Buytaert et al., manuscript submitted). As this cellular response could be responsible for a limited therapeutic response in hypericin-based PDT of bladder cancer, we set out to investigate the molecular mechanism and the signal transduction pathways involved in HO-1 stimulation in our paradigm.

In this report, we present evidence demonstrating that treatment of T24 as well as HeLa cells with hypericin-PDT results in a dramatic induction of HO-1 (Fig. 1(A)), and further confirm that HO-1 has cytoprotective function using pharmacological and RNAi approaches (Figs. 3 and 4). Furthermore, the results of this study demonstrate a cause and effect relationship between p38^{MAPK} activation, HO-1 stimulation and resistance to apoptosis following PDT. This notion is

based on the strong correlation between p38^{MAPK} inhibition and suppression of HO-1 induction (Fig. 2(A)) and increased propensity of the cancer cells to undergo PDT-induced apoptosis when either p38^{MAPK} or HO-1 is knock down (Fig. 4(C),(D)). In previous studies we established that p38^{MAPK} stimulates angiogenic signals following PDT, mainly by promoting the post-transcriptional up-regulation of the COX-2 and the subsequent release of its metabolite PGE$_2$ [5]. However, the mechanism of its anti-apoptotic function remained elusive. Thus the data of this study adds new light into the function of the p38^{MAPK} pathway in our paradigm, by revealing that this stress kinase acts as a key modulator of the cytoprotective HO-1 protein following hypericin-PDT.

The mechanism by which the PI3K pathway positively regulates HO-1 expression in our system is less clear. The combination of p38^{MAPK} and PI3K antagonists resulted in an additive effect both in terms of HO-1 suppression, which was virtually complete when both inhibitors were used together (Fig. 3(B)) and of increased susceptibility to undergo apoptosis in response to PDT (Fig. 3(A)). However when mutated forms of Akt, a major downstream effector of the PI3K pathway, were ectopically expressed in HeLa cells, HO-1 stimulation by PDT was not altered (Kocanova et al., unpublished results). This suggests that PI3K regulates HO-1 expression possibly through an Akt-independent mechanism. In a recent study, Kang and co-workers [23] showed that in response to oxidative stress PI3K regulates HO-1 expression through a mechanism involving actin rearrangement and Nrf2 nuclear translocation, thus raising the intriguing possibility that a similar mechanism operates in our system as well.

Furthermore, this study suggests a functional link between the transcription factor Nrf2 and the signaling pathways regulating HO-1 expression after PDT. This is argued by the observations that Nrf2 nuclear accumulation precedes HO-1 protein expression (Fig. 6(A)), which is abolished by the transcription inhibitor actinomycin D (Fig. 5(A)). Additionally, the same protein kinase antagonists blocking HO-1 stimulation in PDT treated cells, e.g. PD169316 and LY294002, also reduce Nrf2 nuclear accumulation (Fig. 6(B)).

Recent progress have been recently made in the elucidation of the complex mechanisms controlling the Nrf2-Keap1 system, however still many unsolved questions remain as, for instance, whether Nrf2 is degraded in the cytoplasm or in the nucleus and how it accumulates in this sub-cellular compartment following oxidative stress. Different and in some cases contrasting mechanisms have been recently suggested. Oxidation of critical cysteine residues in Keap1 resulting in the inhibition of the Nrf2 degradation pathway, rather than in the dissociation of the Nrf2-Keap1 complex, has been proposed to promote the accumulation of Nrf2 through *de novo* protein synthesis followed by its nuclear translocation [24]. A mechanism implicating direct Nrf2 phosphorylation by endoplasmic reticulum stress-dependent kinase has been suggested to cause dissociation of Nrf2 from Keap1 followed by its nuclear import [25, 26] whereas Nrf2 phosphorylation by protein kinase C at Ser40 disrupted the Nrf2-Keap1 complex but was found dispensable for Nrf2 nuclear accumulation [27]. A recent report proposes that Nrf2 is primarily a nuclear protein and that Keap1 promotes its ubiquitylation and consequent degradation by transiently shuttling in the nucleus [20]. Intriguingly, we also failed by subcellular fractionation to detect Nrf2 in the cytosol (Kocanova et al., unpublished data), at least with the antibody used in this study. Although more experiments are required to fully unravel the molecular mechanism of the Nrf2 activation in photosensitized cells, it is tempting to assume that in our system the p38^{MAPK} and PI3K pathways may connect ROS-induced ER-stress [2] and cytoskeleton perturbations [16] to the Nrf2 nuclear accumulation by regulating Keap1-dependent Nrf2 degradation.

5 Conclusion

In conclusion this report provides evidence indicating that upon photosensitization the activation of the p38^{MAPK} and PI3K signals acts as a molecular sensor of the ROS mediated pathways causing expression of the cytoprotective *ho-1* gene, which likely occurs through a Nrf2-mediated mechanism. As small molecules inhibitors of p38^{MAPK} are clinically available, inhibition of this stress kinase opens an attractive therapeutic strategy in PDT, as it would suppress the expression of HO-1 a powerful anti-oxidant and cytoprotective gene.

References

1. Dolmans DE, Fukumura D, Jain RK (2003) Photodynamic therapy for cancer. Nat Rev Cancer 3:380–387
2. Buytaert E, Callewaert G, Hendrickx N et al (2006) Role of endoplasmic reticulum depletion and multidomain proapoptotic BAX and BAK proteins in shaping cell death after hypericin-mediated photodynamic therapy. FASEB J 20:756–758
3. Agostinis P, Vantieghem A, Merlevede W, de Witte PA (2002) Hypericin in cancer treatment: more light on the way. Int J Biochem Cell Biol 34:221–241
4. Dougherty TJ, Gomer CJ, Henderson BW et al (1998) Photodynamic therapy. J Natl Cancer Inst 90:889–905
5. Hendrickx N, Volanti C, Moens U et al (2003) Up-regulation of cyclooxygenase-2 and apoptosis resistance by p38 MAPK in hypericin-mediated photodynamic therapy of human cancer cells. J Biol Chem 278:52231–52239
6. Volanti C, Hendrickx N, Van Lint J, Matroule JY, Agostinis P, Piette J (2005) Distinct transduction mechanisms of cyclooxygenase 2 gene activation in tumour cells after photodynamic therapy. Oncogene 24:2981–2991
7. Romano M, Claria J (2003) Cyclooxygenase-2 and 5-lipoxygenase converging functions on cell proliferation and tumor angiogenesis: implications for cancer therapy. FASEB J 17:1986–1995
8. Hendrickx N, Dewaele M, Buytaert E et al (2005) Targeted inhibition of p38alpha MAPK suppresses tumor-associated endothelial cell migration in response to hypericin-based photodynamic therapy. Biochem Biophys Res Commun 337:928–935
9. Ryter SW, Alam J, Choi AM (2006) Heme oxygenase-1/carbon monoxide: from basic science to therapeutic applications. Physiol Rev 86:583–650
10. Martin D, Rojo AI, Salinas M et al (2004) Regulation of heme oxygenase-1 expression through the phosphatidylinositol 3-kinase/Akt pathway and the Nrf2 transcription factor in response to the antioxidant phytochemical carnosol. J Biol Chem 279:8919–8929
11. Alam J, Killeen E, Gong P et al (2003) Heme activates the heme oxygenase-1 gene in renal epithelial cells by stabilizing Nrf2. Am J Physiol Renal Physiol 284:F743–752
12. Dennery PA, Visner G, Weng YH et al (2003) Resistance to hyperoxia with heme oxygenase-1 disruption: role of iron. Free Radical Biol Med 34:124–133
13. Gomer CJ, Luna M, Ferrario A, Rucker N (1991) Increased transcription and translation of heme oxygenase in Chinese hamster fibroblasts following photodynamic stress or photofrin II incubation. Photochem Photobiol 53:275–279
14. Nowis D, Legat M, Grzela T et al (2006) Heme oxygenase-1 protects tumor cells against photodynamic therapy-mediated cytotoxicity. Oncogene 25:3365–3374
15. Chen B, Roskams T, Xu Y, Agostinis P, de Witte PA (2002) Photodynamic therapy with hypericin induces vascular damage and apoptosis in the RIF-1 mouse tumor model. Int J Cancer 98:284–290
16. Vantieghem A, Xu Y, Assefa Z et al (2002) Phosphorylation of Bcl-2 in G2/M phase-arrested cells following photodynamic therapy with hypericin involves a CDK1-mediated signal and delays the onset of apoptosis. J Biol Chem 277:37718–37731
17. Jazwa A, Loboda A, Golda S et al (2006) Effect of heme and heme oxygenase-1 on vascular endothelial growth factor synthesis

and angiogenic potency of human keratinocytes. Free Radic Biol Med 40:1250–1263

18. Cheng PY, Lee YM, Shih NL, Chen YC, Yen MH (2006) Heme oxygenase-1 contributes to the cytoprotection of alpha-lipoic acid via activation of p44/42 mitogen-activated protein kinase in vascular smooth muscle cells. Free Radic Biol Med 40:1313–1322

19. Kang KW, Lee SJ, Kim SG (2005) Molecular mechanism of nrf2 activation by oxidative stress. Antioxid Redox Signal 7:1664–1673

20. Nguyen T, Sherratt PJ, Nioi P, Yang CS, Pickett CB (2005) Nrf2 controls constitutive and inducible expression of ARE-driven genes through a dynamic pathway involving nucleo-cytoplasmic shuttling by Keap1. J Biol Chem 280:32485–32492

21. Itoh K, Ishii T, Wakabayashi N, Yamamoto M (1999) Regulatory mechanisms of cellular response to oxidative stress. Free Radic Res 31:319–324

22. Talalay P (2000) Chemoprotection against cancer by induction of phase 2 enzymes. BioFactors 12:5–11

23. Kang KW, Lee SJ, Park JW, Kim SG (2002) Phosphatidylinositol 3-kinase regulates nuclear translocation of NF-E2-related factor 2 through actin rearrangement in response to oxidative stress. Mol Pharmacol 62:1001–1010

24. Kobayashi A, Kang MI, Watai Y et al (2006) Oxidative and electrophilic stresses activate Nrf2 through inhibition of ubiquitination activity of Keap1. Mol Cell Biol 26:221–229

25. Cullinan SB, Zhang D, Hannink M, Arvisais E, Kaufman RJ, Diehl JA (2003) Nrf2 is a direct PERK substrate and effector of PERK-dependent cell survival. Mol Cell Biol 23:7198–7209

26. Cullinan SB, Diehl JA (2004) PERK-dependent activation of Nrf2 contributes to redox homeostasis and cell survival following endoplasmic reticulum stress. J Biol Chem 279:20108–20117

27. Bloom DA, Jaiswal AK (2003) Phosphorylation of Nrf2 at Ser40 by protein kinase C in response to antioxidants leads to the release of Nrf2 from INrf2, but is not required for Nrf2 stabilization/accumulation in the nucleus and transcriptional activation of antioxidant response element-mediated NAD(P)H:quinone oxidoreductase-1 gene expression. J Biol Chem 278:44675–44682

28. Boudrez A, Beullens M, Groenen P et al (2000) NIPP1-mediated Interaction of protein phosphatase-1 with CDC5L a regulator of pre-mRNA splicing and mitotic entry. J Biol Chem 275:25411–25417

29. Assefa Z, Vantieghem A, Declercq W et al (1999) The activation of the c-Jun N-terminal kinase and p38 mitogen-activated protein kinase signaling pathways protects HeLa cells from apoptosis following photodynamic therapy with hypericin. J Biol Chem 274:8788–8796